Published in final edited form as:
Biochim Biophys Acta. 2010 February ; 1804(2): 393. doi:10.1016/j.bbapap.2009.09.031.

Carbonic Anhydrase II-Based Metal Ion Sensing: Advances and New Perspectives

Tamiika K. Hurst[a], **Da Wang**[a], **Richard B. Thompson**[b], and **Carol A. Fierke**[*,a,c]

[a]Department of Chemistry, The University of Michigan, 930 N University Ave, Ann Arbor, MI, USA 48109. Fax: 734 647 4865; Tel: 734 936 2678 [b]Department of Biochemistry and Molecular Biology, University of Maryland School of Medicine, 108 N Greene St., Baltimore, Maryland, USA 21201. Fax: 410 706 7122; Tel: 410 706 7142; rthompso@umaryland.edu [c]Department of Biological Chemistry, The University of Michigan, 930 N University Ave, Ann Arbor, MI, USA 48109. Fax: 734 647 4865; Tel: 734 936 2678; fierke@umich.edu

Abstract

Carbonic anhydrases are archetypical zinc metalloenzymes and as such, they have been developed as the recognition element of a family of fluorescent indicators (sensors) to detect metal ions, particularly Zn^{2+} and Cu^{2+}. Subtle modification of the structure of human carbonic anhydrase II isozyme (CAII) alters the selectivity, sensitivity, and response time for these sensors. Sensors using CAII variants coupled with zinc-dependent fluorescent ligands demonstrate picomolar sensitivity, unmatched selectivity, ratiometric fluorescence signal, and near diffusion-controlled response times. Recently, these sensors have been applied to measuring the readily exchangeable concentrations of zinc in the cytosol and nucleus of mammalian tissue culture cells and concentrations of free Cu^{2+} in seawater.

Keywords

carbonic anhydrase; zinc; copper; biosensor; fluorescence

Role of Zinc in Biology

Transition metals, including zinc, copper, iron and nickel, are essential minerals for living organisms. Zinc, the second most abundant trace element after iron, plays important catalytic, structural, and regulatory roles in cells. Bioinformatic analysis indicates that 3%–10% of the human genome encodes potential zinc binding proteins [1]. More than 300 zinc enzymes covering all six classes of enzymes have been discovered (reviewed in [2], [3], [4]); in many cases, the zinc ion is an essential cofactor for the observed biological function of these metalloenzymes. Carbonic anhydrase was the first zinc-dependent enzyme discovered [5]. Additionally, various zinc-binding motifs that are important for stabilizing protein structure mediate diverse biological processes [6].

[*]The authors thank the National Institutes for Health GM40602 (to CAF) the National Institute of Biomedical Imaging and Bioengineering 1 RO1 EB03924 (to R.B.T.) for support.

Disturbance of zinc homeostasis can cause multiple disorders in human health. Humans require a daily intake of several mg of zinc to maintain normal zinc levels [7]. Zinc deficiency, resulting from either genetic defect or dietary limitation, causes growth retardation, lethargy, gastrointestinal disorders, dermatological lesions, defects in reproductive organs, and dysfunction of the immune system [8]. Loss of function in zinc absorption transporters in the small intestine causes severe zinc deficiency and death in utero [9]. Furthermore, increased vulnerability to infections is the leading cause of death among zinc-deficient populations in developing countries [10]. Zinc supplementation has successfully been used as a treatment of many disorders, including acrodermatitis enteropathica (inflammation of the skin and the small intestine), age-related macular degradation and pediatric diarrhea [11]. Accumulating evidence also supports a role for zinc in the development of chronic diseases such as Alzheimer's disease, diabetes, and asthma [12]. Excess zinc can induce aggregation of amyloid-β and formation of plaque [13], the hallmark of Alzheimer's disease, and oral administration of zinc chelators substantially reduces the plaque formation in mouse models [14]. Decreased serum zinc levels are seen in Type I diabetes patients, and dietary supplementation with zinc reduces the incidence of chemically-induced diabetes in mice [15]. Furthermore, a missense mutant of the zinc transporter (ZnT8), believed responsible for inserting zinc into pancreatic beta cell insulin-containing vesicles, was identified as a risk factor for Type 2 diabetes [16]. Therefore, development of methods to better understand zinc homeostasis in cells and organs should have implications for the treatment of a number of diseases.

Methods to measure total metal concentrations

A wide variety of analytical techniques are available for the determination and quantitation of metal ions in solutions. Measurement of low concentrations of analytes in complex media, like seawater and blood, is increasingly important for both biomedical and environmental applications. In particular, determination of the concentrations of transition metals, including copper and zinc, is of great interest as these metal ions are essential for human health and can be toxic at elevated levels.

Unlike iron or copper, zinc contains a filled d orbital ($3d^{10}4s^{0}$) and therefore is not amenable to direct determination by optical absorption, emission, electron paramagnetic resonance, or related techniques. Therefore, techniques such as atomic absorption spectroscopy, mass spectrometry and X-ray absorption spectroscopy have been employed to measure zinc. Hybrid techniques (i.e. HPLC-atomic absorption spectroscopy, ICP-MS), in which separation of the species of interest is coupled with a metal specific detector, have been established as reliable and robust analytical tools for analysis of multiple metal ions in biological and environmental applications [17,18]. The separation component of the coupled system is important when the target analytes have related chemical properties. The choice of the detector depends on both the analyte concentration, and the required limit of detection. Because of its multi-element capability and low detection limits, inductively coupled plasma mass spectrometry (ICP-MS) is the most widely used method to measure the concentration of a given metal in complex mixtures [18]. Like all analytical techniques, ICP-MS has inherent limitations. First, the sample is destroyed during metal analysis. Second, ICP-MS measures the total metal concentration in a sample irrespective of the speciation of that metal, whereas in biological or environmental matrices it is often the concentration of the readily exchangeable or bio-available metal ion that is of interest. Finally, ICP-MS cannot be used for real-time intracellular monitoring of metals. Therefore, additional methods to quantify zinc concentrations are needed.

New methods to measure and image metals in biological samples are under development. Recently X-ray fluorescence spectrometry (XRF) has been employed to measure and image metal ions in cells and tissues [19]. XRF is a nondestructive method for the elemental analysis of solids and liquids, but is destructive to cells and typically requires dehydration of the sample

prior to imaging. In this method, the sample is irradiated by an intense x-ray beam that causes the emission of fluorescent x-rays from inner shell electrons of metal ions. The spectrum of emitted x-rays is detected using either an energy dispersive or wavelength dispersive detector. The elements in the sample are identified by the wavelengths of the emitted x-rays, while the concentrations of the elements are determined by the intensity of those x-rays in comparison to standards [20]. This technique allows for simultaneous detection of >10 elements with detection limits typically varying between 10 and 100 ppm dry weight, depending on the elements to be analyzed and the sample matrix [21]. X-ray fluorescence has been useful for imaging metal ions within cells [22]; coupling XRF with traditional light microscopy allows the coupling of cell morphology with in vivo metal ion distribution. Like ICP-MS, an issue with XRF imaging is that quantitation is based on the total metal content and not the free metal ion concentration.

Methods to measure “free” metal concentrations

The methods above allow for the measurement of the total metal concentration in a sample. However, zinc in biological systems is bound to myriad proteins and small molecules, thereby decreasing the “free” or readily exchangeable metal concentration by orders of magnitude and complicating analyses. Consequently, fluorescence methods based on indicators whose emissions respond to bound metal have become the most prevalent approach for quantifying many divalent metals in both aqueous and biological samples. Fluorescent sensors are classified according to the receptor molecule and the fluorescent signal. If the transducer is a molecule that is biological in origin, the sensor is called a biosensor (Figure 1). The success of fluorescent sensors in biology has been due in part to their ability to correlate analyte concentration distributions with the physical structures of cells and tissues. An array of fluorescent, zinc-selective chelators have been developed and applied to zinc measurements (recently reviewed in [23], [24], [25], [26]). Many desirable traits of fluorescent metal ion indicator systems are now apparent. Perhaps the most important consideration is high affinity and selectivity for zinc or other target metal ions; the probe must not only respond to free zinc but reject potentially interfering metal ions present at up to billion-fold higher concentrations. Metal selectivity has been a limitation of many fluorescent sensors; these chelators often retain affinity for ions such as Ca^{2+} and Mg^{2+}. While calcium or magnesium do not produce interference when present at equal concentrations with zinc, intracellular concentrations of these metals are significantly higher than that of free zinc [27], [28], [29], and therefore can interfere by saturating all of the metal binding sites of the fluorophore. To quantify zinc concentrations in real-time, zinc should equilibrate with the sensor; therefore metal binding should be fast, reversible, and ideally of 1:1 stoichiometry. Furthermore, the sensor should have a metal affinity comparable to the free metal concentration. Reliable quantitation is essential for many studies, so a wavelength ratiometric, polarization, or lifetime response is necessary. A sensor where the analyte binding only induces a change in fluorescence intensity is of modest use for quantitation because so many other factors can also cause apparent intensity changes, including: changes in the probe concentration due to photobleaching or washout, variations in the excitation intensity or sample thickness, the presence of adventitious quenchers, and so on. The potential for these artifacts led to the introduction of wavelength ratiometric indicators for pH and calcium [30], and later lifetime- [31], [32] and polarization-based chemical analyses [33], all of which are largely free of these artifacts. An excitation wavelength in the visible range or near IR is preferred so as to reduce damage to the cell and confounding autofluorescence. For both in vitro and in vivo intracellular applications, solubility and membrane permeability are vital; furthermore, washout and nonspecific binding (e.g., to proteins) must be minimal. The optimal properties of fluorescent sensors can depend on the proposed use for the sensor.

Specific tools for monitoring Zn^{2+}

Among the most important tools for studying the roles of metal ions such as Zn^{2+} in biology have been metallofluorescent indicators (sometimes called sensors). These indicators recognize the presence of the free metal ion and indicate it as a change in fluorescence, which can be measured or photographed. The change may be in the intensity (either enhancement or quenching), the excitation or emission wavelength, or in a few cases, the polarization or lifetime of the fluorescence [34], [35], [36]. There are several advantages to the fluorescence approach for studying metals in biology. First, the fluorescence can be imaged in cells, tissues, or living organisms, which enables the analyte distribution to be related to the structure of the living cell or organism. Most imaging is done in the microscope, which permits the use of small samples. Second, in good examples the indicators are quite sensitive and specific for the analyte, and respond rapidly enough to follow physiologically important processes. Third, in some cases the indicators permit quantitative determination of the analyte in situ, without sample collection or processing, which may be infeasible on a subcellular level. Fourth, by using protein or organelle-specific fluorescent stains and other indicators emitting at different wavelengths, the analyte level may be spatially related to a specific structure or organelle, or the distribution of another analyte in the cell. Finally, imaging or scanning can be used to screen a large number of specimens at high rates for fluorescence changes, which is routinely used to test candidate drugs for efficacy in treating disease. For all these reasons, hundreds of fluorescent indicators and stains have been developed for diverse purposes.

Scores of fluorescent indicators have been described for measuring zinc ion in solution and excellent reviews have appeared recently [25], [24], [25], [26]; unfortunately, the scope of this article necessitates the omission of much important work. Most of these indicators are small organic fluorophores that also have multiple chelating moieties, such as amines or carboxylates, capable of binding the metal ion. Early indicators (such as 8-hydroxyquinoline) were mostly ill-suited for studying biological systems mainly due to a lack of specificity for zinc compared to other metal ions more prevalent in biological matrices, such as calcium and magnesium [34], [35]. Frederickson developed the first zinc indicator widely used for biological specimens (TSQ: N-6-methoxy-8-quinolyl)-p-toluenesulfonamide), which served as an histological stain for granular zinc in brain, pancreas, and other tissues [37]. However, the pH-dependence and insolubility of the 2:1 complex made TSQ poorly suited for soluble zinc and quantitation problematic. Several important advances appeared with the introduction of the more soluble Zinquin [38], including exploitation of dequenching by binding amine moieties [39], higher selectivity zinc binding moieties [40]; ratiometric response [41]; targeting to mitochondria [42] and high affinity [43], [44]. A significant proportion of these indicators are available commercially and, where appropriate, widely used. While the development of these indicators has come a long way, no indicator or family of indicators offers high (or tunable) affinity, ratiometric or other accurate quantitation, rapid response, and targeting to desired cell types and/or organelles.

Knowing the high selectivity with which biomolecules, such as proteins, bind metal ions, several workers constructed peptides or proteins with biomimetic metal ion binding sites and transduced the binding as changes in fluorescence using attached labels [45], [46], [47]. These indicators may be termed “biosensors” because of their use of biologically-derived molecules for recognition of the analyte. Other investigators drew on the pioneering work of Miyawaki in developing FRET-based sensors [48], where the binding of zinc ion to a protein induces a conformational change, bringing two tethered fluorescent protein moieties closer together, thereby improving their energy transfer efficiency [49], [50], [51]. While these approaches have been promising (particularly the prospect of an expressible indicator), until recently [52] they had not demonstrated the high affinity and selectivity observed for natural metal ion

binding sites. As will be seen, the CA-based biosensors offer all these desirable traits, and more.

Carbonic Anhydrase

Meldrum and Roughton discovered a new enzyme present in red blood cells that catalyzed the reverse hydration of CO_2 to HCO_3^- [53], [54]. This enzyme, named carbonic anhydrase, was identified as the first zinc metalloenzyme. For both the in vivo function and the use of CA in sensors, the affinity and selectivity of metal ion binding to the active site is key. The crystal structure of human CAII demonstrates that the active site, located in the central region of a ten stranded, twisted β-sheet, is comprised of a cone shaped cleft, 15 Å deep, with a tetrahedral Zn^{2+} ion at the bottom of the cleft [55], [56]. The imidazole side chains of three histidine ligands, at positions 94, 96 and 119, are directly coordinated to the metal center (Figure 2). These direct ligands form hydrogen bonds to the indirect ligands Gln-92, Asn-244 and Glu-117, respectively. Filling out the coordination sphere of zinc is a hydroxide ion that forms a hydrogen bond to Thr-199 at neutral pH. With the exception of Asn-244, which is hydrogen bonded to His-96 through the main chain carbonyl oxygen, the direct and indirect metal ligands are invariant in all sequenced catalytically active α-carbonic anhydrases [57], [58]. This prototypical metal site is completed by hydrophobic residues that surround the zinc site. By comparison, the beta class of carbonic anhydrases contains a $HisCys_2H_2O$ zinc polyhedron [59].

Determinants of metal affinity of CAII

Metal affinity is determined by optimal interactions between the CAII metal ligands and the bound metal ion. The nature of the metal ligands, the hydrogen bond network and the hydrophobic shell all contribute to the picomolar metal affinity of CAII [55], [56]. Large changes in metal affinity occur by altering the number of metal ligands. Substitution of one of the histidine side chains with alanine decreases the metal affinity by at least 10^5-fold (Figure 3), while introduction of a fourth ligand into the metal coordination sphere of CAII by replacing T199 with Glu, Asp or Cys increases the affinity up to 100-fold [60], [61]. Spectroscopy and crystallography demonstrate that the new thiolate side chain coordinates to the metal ion, displacing the metal-bound solvent molecule. Furthermore, substitution of any of the His ligands with another side chain capable of coordinating the zinc ion, such as Asp, Glu, Gln, Asn or Cys, substantially decreases zinc affinity [62], [63], [64], [65], [66]. Crystal structures of these variants demonstrate that none of these side chains position the coordinating atom at the same place as the imidazole nitrogen, leading to movements in the location of the bound zinc ion.

Deletion of any one of the hydrogen bonds with the second shell ligands also reduces zinc affinity although this effect is more modest, decreasing zinc affinity 10 – 40-fold [67], [68]. Thermodynamic measurements of metal binding demonstrate that modifications in the metal polyhedron of CAII lead to a complex series of changes in both the enthalpy and entropy of ligand binding that is most readily rationalized in terms of metal and protein desolvation, rather than in terms of changes in the direct interactions of ligand and protein [69]. Although the second shell ligands were proposed to function primarily by orienting the direct ligands, mutations in these residues produce profoundly different effects on the enthalpy of binding, depending on the nature of the residue. These results indicate that the second shell ligands make both enthalpic and entropic contributions to metal binding.

Finally, alterations in the hydrophobic residues (Phe-93, Phe-95 and Trp-97) underneath the zinc binding site decrease the metal affinity of CAII by as much as 100-fold [70], [71]. Crystal structures of these mutant proteins demonstrate alterations in the structure of the apo-enzyme such that the histidine side chains are no longer correctly oriented to bind zinc [72]. In addition

to providing fundamental insight into the determinants of metal affinity, the metal affinity of these CAII variants span the range from subpicomolar to micromolar thereby providing an array of CAII proteins that could be used to measure a wide range of zinc concentrations.

Kinetics of Zinc ion binding to CAII

In CAII, zinc equilibration is limited by both the high zinc affinity (pM) and the slow dissociation rates. The measured association rate constant at ~10^5 M^{-1} s^{-1} is much slower than a diffusion-controlled limit of $10^{7-}10^8$ M^{-1} s^{-1} leading to a half-time for dissociation estimated at several months [67], [73], .The slow association rate constant suggests that metal binding occurs in a two-step mechanism: formation of an initial complex followed by a conformational change (Scheme 1). The apparent association rate constant increases significantly for mutants with one of the histidine ligands replaced with alanine (His_2 zinc site) or the second shell hydrogen bond between His119 and E117 removed (E117A mutant) [64], [67]. These mutations suggest that the kinetic mechanism for zinc binding occurs via an intermediate where the zinc ion is bound to the two ligands nearest the active site surface, His94 and His96, followed by slow addition of the third His ligand (H119) and dissociation of water ligands to form the tetrahedral metal site (Scheme 1; [67]). The E117A mutation has proven particularly useful for zinc sensing since this mutation decreases the half-time for zinc dissociation by 5000-fold while only decreasing the zinc affinity by 40-fold [67].

Equilibration of CAII with zinc can be facilitated by the addition of certain chelators, including dipicolinic acid (DPA) [74], [75], but not others, including EDTA. Catalysis of metal exchange by DPA is proposed to occur by the formation of a CAII-DPA-Zn^{2+} ternary complex (Scheme 2); the apparent association rate is increased because CAII binds DPA-bound Zn^{2+} which is in higher concentration than the “free” zinc and the dissociation rate constant is enhanced by the bound DPA [75]. This type of chelator-catalyzed zinc exchange could mimic intracellular mechanisms that are proposed to enhance zinc equilibration [29], [76].

Metal Specificity of CAII

Through evolution the structure of CAII has been selected to bind Zn^{2+} in the presence of a variety of potential cellular interferents, including: Mg^{2+} (estimated free concentration of 0.5–1 mM) [27], Ca^{2+} (est. free concentration of 0.05–1 μM) [28], [77], [78] Fe^{2+} (est. free concentration of 0.1–10 μM) [79], [80], [81], [82], and Cu^{2+} (est. free concentration of ~ 10^{-18} M [83].) Like small molecule ligands, the metal affinity of wild type CAII follows the Irving-Williams series (Mn^{2+} <Co^{2+} <Ni^{2+} <Cu^{2+} >Zn^{2+}) although the zinc affinity is increased significantly compared to the rest of the transition metals (Figure 4) [66], [84], [85]. Copper could potentially compete with zinc for binding to CAII in a cell since the affinity is 10-fold higher than zinc; however, the readily exchangeable copper concentration is estimated at >>1000-fold lower than that of zinc [86]. CAII has little affinity for other possible competitors; the dissociation constant of CAII for Ca^{2+} and Mg^{2+} is larger than 10 mM and the affinity of Fe^{2+} is estimated to be significantly higher than 100 μM [85]. Therefore, CAII has significantly higher metal selectivity compared to small molecule chelators such as EDTA, NTA, DPA and TPEN that have little discrimination in binding affinity between Co, Ni, Zn and Cd (Table 1).

Structures of metal-substituted CAII enzymes reveal that the geometry of the metal site often varies with the identity of the metal. For example, copper binds to wild-type CAII in a trigonal bipyramidal geometry, accepting an additional water as a ligand while both bound manganese and nickel are octahedral with three water molecules [56], [87]. The enthalpy of metal binding to CAII decreases through the series Co^{2+} Zn^{2+}→Cu^{2+}, mirroring the enthalpy of hydration, suggesting that desolvation of the metal ion plays an important role in metal affinity and selectivity [88].

The metal selectivity of CAII is also determined by the structure of the active site. Mutagenesis of the His ligands to another side chain capable of coordinating Zn^{2+}, including Asp, Glu, Gln, Asn, and Cys, leads to CAII variants with altered metal selectivity [66]. For example, the selectivity for zinc compared to copper (K_{Zn}/K_{Cu}) varies from 0.1 to 2×10^{-4} to 15 for wild-type, H119N, and H119Q CAII, respectively (Figure 5). Similarly, the selectivity for zinc compared to nickel (K_{Zn}/K_{Ni}) varies from a value of 2×10^4 for wild-type CAII to 1 for the H94D mutant. Nonetheless, except for H119Q CAII, the metal selectivity of all of these mutants follows the inherent metal ion affinity trend suggested by the Irving-Williams series, demonstrating the importance of this trend for metal ion selectivity in biology. Furthermore, neither the polarizability of the liganding side chains nor the size of the metal ion binding site correlate strongly with metal ion specificity; instead, changes in metal ion specificity in the variants correlate with the preferred coordination number and geometry of the metal ion [58]. This correlation suggests that a primary feature driving deviations from the inherent ligand affinity trend is the positioning of active site groups such that a given metal ion can adopt a preferred coordination number/geometry.

The hydrophobic residues underneath the zinc binding site in CAII also contribute to metal selectivity. As the hydrophobicity and size of the amino acids at positions 93, 95 and 97 decrease, the affinity of CAII for metal ions that bind with a tetrahedral geometry, $zinc^{2+}$ and $cobalt^{2+}$, decreases [71,89]. In contrast, the affinity of CAII for the trigonal bipyramidal Cu^{2+} increases significantly. These two trends contribute to the enhanced copper selectivity for these mutants with values of K_{Cu}/K_{Zn} as high as 10^6. A comparison of the crystal structures of the apo forms of wild-type and F93I/F95M/W97V CAII demonstrates that mutations in the hydrophobic residues disrupt the positioning of the His ligands in a tetrahedral geometry in the absence of bound metal [72]. Therefore, this hydrophobic shell is important for stabilizing the tetrahedral metal ion geometry for zinc and destabilizing alternative geometries, such as the trigonal bipyramidal geometry of copper.

CA-based zinc sensing: ratiometric fluorescent sensors

Most of the CA-based zinc sensors rely on the zinc-dependent binding of a ligand to the protein. Aryl sulfonamides have long been known to inhibit holo-carbonic anhydrase [90]. Hundreds of these compounds with various structural properties and activity have been identified, some of which are being used to treat glaucoma. The mechanism for inhibition is well-understood; aryl sulfonamides contain the weakly acidic SO_2NH_2 moiety that directly coordinates the zinc ion through the ionized NH^- group, displacing the zinc bound water [91]. The first approach to fluorometrically determine zinc using carbonic anhydrase as a recognition element evolved from the work of Chen and Kernohan [92]. They discovered that the fluorescence emission of the aryl sulfonamide, dansylamide (DNSA), upon binding to holo-carbonic anhydrase is both enhanced significantly and blue-shifted. Thompson and Jones [93] determined that DNSA has very weak affinity for apo-CA and thus the fraction of CA with bound DNSA reflects the fraction of zinc-bound CA, which is determined by the free zinc concentration. Therefore the ratio of emissions from free and bound dansylamide could be used to determine the free zinc concentration. To optimize CA-based fluorescence sensors for accurate quantitation, the metal ion binding has been transduced using wavelength ratiometric indicators as well as lifetime- and polarization-based methods [94], [95], [96], [97]. Wavelength ratiometric measurements have been applied to quantification of free zinc in biological samples. Zinc release from brain cells in a rabbit ischemia model was measured by adding apo–CA to the dialysate in the brain of a living rabbit and then quantifying zinc concentrations from the fluorescence emission ratio after addition of DNSA [98]. Similarly, neuronal zinc release from organotypic cultures of mammalian hippocampus following electrical stimulation was measured using apo-CAII and a water-soluble aryl sulfonamide, ABD-N, with an improved extinction coefficient and a longer excitation wavelength [94]. In both of these cases the exchangeable zinc concentrations (1–

100 nM) are much higher than the K_{Zn} for CAII (1 pM), therefore the measurements were carried out using high concentrations of apo-CAII and sulfonamide (1–20 μM) such that zinc binds to CAII stoichiometrically. In this linear relationship, the detection limit is established by the lowest fractional occupancy that can be reliably measured, which is usually considered as 0.1%; therefore, the dynamic range is thus largely determined by the concentration of apo-CAII. Stoichiometric methods depend on accurate knowledge of the concentration of CAII and maintaining an excess concentration of both CAII and sulfonamide. Therefore, stoichiometric methods do not work for in vivo measurements where the total zinc concentration is high (~0.2 mM) and well buffered by numerous ligands and consequently difficult to deplete.

To address these issues, an excitation ratiometric method was developed based on Förster resonance energy transfer (FRET) [99] between a cell-permeable sulfonamide, Dapoxyl sulfonamide, and a second fluorophore attached to CAII (Figure. 6) [100]. The fluorophore that is covalently attached to CAII serves as a FRET acceptor for the bound sulfonamide, such that emission from the bound sulfonamide is efficiently transferred to the label on the protein, which emits at much longer wavelengths. In this case, the label is AlexaFluor594 maleimide (AF594, Ex 594/Em 617) that is attached to the thiol group of a unique cysteine (H36C/C206S) engineered on the surface of CAII; the position of the label on CA and the overlap of its absorbance with the emission of Dapoxyl sulfonamide are chosen so that energy transfer from the sulfonamide to the AF594 is nearly quantitative. For this sensor, when Dapoxyl sulfonamide bound to AF594-CAII is excited at 365 nm, fluorescence emission is observed at 617 nm from the AF594 because of FRET. Thus the UV-excited red emission (Ex 365 nm/Em 617 nm) represents the fraction of AF594-CAII with sulfonamide (and therefore zinc) bound, whereas the signal of the directly excited AF594 (Ex 548 nm/Em 617 nm) represents the total amount of the AF594-CAII. The fluorescent ratio of UV excited (365 nm) to directly excited (548 nm) emissions correlates with the zinc-bound fraction of the sensor and thus free zinc. In vivo calibrations are carried out using a series of nitrilotriacetic acid (NTA)-chelated zinc buffers in which the free zinc concentration is maintained at a fixed level, indicating that the apparent zinc affinity of this sensor is ~140 pM. An important advantage of this approach is the relative insensitivity to the sulfonamide level, sulfonamide bound to membranes and proteins, and adventitious holo-CA present in the specimen, since only the fraction of the sulfonamide in close proximity (effectively, bound) to the labeled CAII is observed. Also, even though UV excitation is used, the large difference between the excitation and emission wavelengths leads to a very low autofluorescence background.

This sensor was applied to measure the intracellular free zinc concentration in the mammalian cell line PC-12 under resting conditions [29]. Because AF594-CAII is ordinarily cell-impermeant, an 11 amino acid cell-permeating peptide (TAT-tag derived from HIV-1 protease) was fused to the N-terminus to facilitate uptake [101]. Using this method, the concentration of free zinc is measured at 5–10 pM compared to a standard curve and assuming equilibration between CAII and the readily exchangeable zinc concentration. To examine whether zinc equilibration in vivo occurs readily despite the slow zinc association rate constant in vitro, we demonstrated that the measured zinc concentration is not dependent on the concentration of sensor or on the equilibration time (20 min to 24 hr). Furthermore, the same “free” zinc concentration in PC12 cells is observed using the AF594-labeled E117A CAII mutant as the receptor molecule where the zinc equilibration rate is increased by 800-fold [102]. The picomolar affinity of this CAII sensor is the most sensitive sensor used to measure cellular zinc to date.

In addition to measuring the readily exchangeable zinc concentration, these data have further implications for the mechanism of cellular zinc homeostasis. First, these data indicate that there is a substantial exchangeable zinc pool in the cell; the concentration of the CAII sensor is in the nanomolar regime providing a lower limit for the exchangeable zinc pool. Since the total

zinc concentration in cells is ~0.2 mM, an exchangeable zinc pool in the nanomolar to micromolar range is still a small percentage of the total cellular zinc. Second, the rapid equilibration of the sensor with the readily exchangeable zinc concentration is inconsistent with the CAII sensor binding the picomolar "free" zinc with the 10^5 M^{-1} s^{-1} association rate constant measured in vitro since the estimated equilibration half-time for this reaction is on the order of several hours. These data suggest that zinc may bind to CAII via a zinc-chelator complex in vivo, where the chelator is either a small molecule or protein chaperone, perhaps similar to the mechanism of DPA-catalyzed zinc binding to CAII (Scheme 2). In summary, these data indicate that there is a readily exchangeable pool of cellular zinc that equilibrates rapidly with zinc-binding proteins such as carbonic anhydrase.

Carbonic anhydrase with wild-type zinc affinity is ideal for measuring the cellular zinc concentration under equilibrium conditions for most cells. However, free zinc concentrations in neuronal models vary over 7 orders of magnitude from 10 pM in normal resting cells to more than 10 μM outside the neurons after stimulation of synaptic zinc release [29], [103], [104]. To measure zinc concentrations over this wide dynamic range, CAII receptors with altered zinc affinities, such as CAII mutants described previously (Figure 5) will be of great utility [105].

Expressible ratiometric CA-based sensors

Although TAT-tag mediated delivery of ratiometric CA sensors has been successfully applied to mammalian cell lines, it cannot penetrate some other organisms without detrimental effects [106]. Also, the chemical labeling of the isolated protein with the AlexaFluor fluorophore is tedious, labor intensive, and does not always proceed in high yield. A further improvement in zinc sensors would be to further develop and optimize a protein-based sensor that can be readily expressed in cells [107], [108]. The expressible sensor can be constructed by fusing a fluorescent protein to CAII as a fluorescence acceptor and using a zinc-dependent FRET donor, like the Dapoxyl sulfonamide used in the previous sensor. The relatively small size of the fluorescent protein variants and CAII generally means that efficient energy transfer between the Dapoxyl sulfonamide and the fluoresecent protein acceptor is feasible. An ideal candidate fluorescent protein for an expressible CA sensor should meet the following criteria: excitation spectrum overlap with the emission of Dapoxyl sulfonamide to ensure good FRET efficiency, high extinction coefficient and quantum yield, fast maturation, and monomeric state. Directed evolution studies have generated a large pool of fluorescent proteins that can be used for this purpose [109], such as variants of RFPs from Discosoma sp. and Entacmaea quadricolor [110], [111], [112]. Furthermore, fluorescent proteins with different spectra can be coupled to CA variants with different zinc affinities, thus creating a multicolor measurement covering a wide dynamic range in a single experiment. Our initial experiments have used DsRed2 and mCherry [112] in fusion proteins; this work is ongoing, including the use of sequences to target the expression to particular organelles within the cell.

Other Zn sensing methods using CAII

Fluorescence anisotropy is another ratiometric approach that provides an accurate alternative for quantification, especially for fluorophores with smaller changes in lifetime and quantum yield. In some cases fluorescence anisotropy offers a particular advantage of an expanded dynamic range, as observed for the carbonic anhydrase-based sensor [113], [114], [115]. Fluorescence anisotropy-based sensing has not been widely used for cellular studies, perhaps because fluorescence polarization microscopes are less common than those permitting wavelength ratiometric determinations of analytes.

CA-based sensors can also be used to measure zinc concentrations based on changes in fluorescence lifetime. Fluorescent aryl sulfonamides, including dansylamide and Dapoxyl sulfonamide, exhibit substantial changes in their average fluorescence lifetimes upon binding

to holo-CA, consistent with the increases in the apparent quantum yield [92], [97]. Using standard time- or frequency-domain methods, the proportions of the lifetimes corresponding to the free and bound forms of the sulfonamide can be determined, and therefore, the free zinc concentration can be calculated in the same manner as for the wavelength ratiometric approaches. Lifetime-based methods have advantages similar to those of ratiometric determinations; however, microscopes capable of imaging fluorescence lifetimes are still uncommon [116].

Environmental Applications using CAII-based Sensors

CAII-based sensing has also been applied to the determination of metal ions, such as Cu^{2+} and Zn^{2+}, in natural waters. Cu^{2+}, Zn^{2+}, and to a lesser extent Cd^{2+}, Co^{2+}, and Ni^{2+} are of interest environmentally for two main reasons. First, Cu and Zn are nutrients required by essentially all organisms, and their availability (together with Fe) in natural waters effectively controls the growth of phytoplankton and thus all other organisms in the food chain as well. As a consequence, Cu and Zn typically exhibit a “nutrient distribution” in the ocean, with low levels in the sunlight-exposed photic zone near the surface, and elevated concentrations at greater depth [117]. Second, Cu and Zn at elevated levels are toxic to many life forms, and are thus important pollutants in many harbors and estuaries [118]. For instance, the blue mussel, a commercially important shellfish, is killed by Cu^{2+} at sub-ppb levels [119]. Speciation of metal ions in natural waters (e.g., the proportion of total metal bound to different ligands, particles and colloids in a sample) is important, because it determines the availability of the metal ions to various organisms; conversely, the marine biota have a dramatic influence on the speciation and distribution of biologically important metals [117], [120]. The importance of these questions has led to substantial study of the marine geochemistry of these metal ions.

Copper sensing using CAII is based on copper binding to the His_3 metal site and quenching the fluorescence of a fluorophore, such as Oregon Green, that is covalently attached to a unique Cys residue near the metal site, such as L198C [121]. Copper binding to fluorophore-labeled CAII results in a concomitant decrease in fluorescence intensity and lifetime, the latter of which results in increased modulation and decreased phase angle [122], [123] (Figure 8). The free Cu^{2+} concentration can be determined under equilibrium conditions from the observed lifetime or phase angle in comparison to a standard curve. The CAII variants with altered copper affinity and enhanced copper selectivity will be useful for limiting interference from Zn and for measuring a variety of copper concentrations. Other metal ions such as Co^{2+}, Cd^{2+}, and Ni^{2+} also exhibit quenching of suitably positioned fluorophores upon binding to the active site of CA and can be quantified by changes in fluorescence intensity, lifetime, or fluorescence polarization [95].

The high sensitivity and selectivity of CA-based fluorescence sensors for zinc and copper are well suited to determining free metal ions in the complex matrix of sea water. CA-based sensors offer some unique advantages in comparison to other methods of determining free metal ion concentration (and thus speciation). First, compared to CA-based sensing, existing (mainly voltammetric) methods of determining free Cu^{2+} and Zn^{2+} in sea water are relatively slow and labor intensive, such that only a few samples a day can be analyzed by a skilled practitioner [124], [125], [126]; by comparison, CA-based sensors can determine these metals in sea water without any processing or separation steps, and can also act as a true sensor, providing a continuous readout of metal ion concentration in situ, in real time [127]. Also, the fluorescent-labeled CAII can be immobilized at the end of an optical fiber, which can be immersed and the metal ion concentration determined remotely in situ at some depth in the water column [116]. This is of importance since collecting water samples is slow and expensive, and risks contamination of the samples compared with determination in situ with a fiber optic sensor. In

view of the power and flexibility of the CA-based fluorescence sensors, we anticipate they will find many uses in environmental monitoring of metal ions.

Conclusions and future work

CAII-based sensors have been demonstrated to quantify readily exchangeable zinc concentrations in mammalian cells and "free" Cu^{2+} concentration in seawater. These sensors have a bright future for examining zinc concentrations and changes in zinc concentrations in a wide variety of cells and subcellular organelles as well as in tissues. The ability to measure readily exchangeable zinc concentrations using CAII-based sensors is an important new tool for answering biological questions concerning intracellular zinc storage and distribution, the role of zinc in signaling pathways as well as the pathological roles of zinc in human disease. In the future, this sensor may also find important applications in measuring the readily exchangeable concentration of other metal ions, including copper, in cells and in seawater.

Abbreviations

CAII	carbonic anhydrase isozyme II
ICP-MS	inductively coupled plasma mass spectrometry
XRF	X-ray fluorescence spectrometry
FRET	Förster resonance energy transfer
TSQ	N-6-methoxy-8-quinolyl)-p-toluenesulfonamide
DNSA	dansylamide
AF594	AlexaFluor594
NTA	nitrilotriacetic acid

References

1. Andreini C, Banci L, Bertini I, Rosato A. Counting the zinc-proteins encoded in the human genome. J Proteome Res 2006;5:196–201. [PubMed: 16396512]
2. Coleman JE. Zinc proteins: Enzymes, storage proteins, transcription factors, and replication proteins. Annual Review of Biochemistry 1992;61:897–946.
3. Christianson DW. Structural biology of zinc. Advances in Protein Chemistry 1991;42:281–355. [PubMed: 1793007]
4. Vallee BL, Auld DS. Zinc coordination, function, and structure of zinc enzymes and other proteins. Biochemistry 1990;29:5647–5659. [PubMed: 2200508]
5. Keilin D, Mann T. Carbonic anhydrase. Purification and nature of the enzyme. Biochem J 1940;34:1163–1176. [PubMed: 16747299]
6. Matthews JM, Sunde M. Zinc fingers--folds for many occasions. IUBMB Life 2002;54:351–355. [PubMed: 12665246]
7. Maret W, Sandstead HH. Zinc requirements and the risks and benefits of zinc supplementation. J Trace Elem Med Biol 2006;20:3–18. [PubMed: 16632171]
8. Vallee BL, Falchuk KH. The biochemical basis of zinc physiology. Physiological Reviews 1993;73:79–118. [PubMed: 8419966]
9. Liuzzi JP, Cousins RJ. Mammalian zinc transporters. Annu Rev Nutr 2004;24:151–172. [PubMed: 15189117]
10. Tuerk MJ, Fazel N. Zinc deficiency. Curr Opin Gastroenterol 2009;25:136–143. [PubMed: 19528881]
11. Bhandari N, Bahl R, Taneja S, Strand T, Molbak K, Ulvik RJ, Sommerfelt H, Bhan MK. Substantial reduction in severe diarrheal morbidity by daily zinc supplementation in young north Indian children. Pediatrics 2002;109:e86. [PubMed: 12042580]

12. Devirgiliis C, Zalewski PD, Perozzi G, Murgia C. Zinc fluxes and zinc transporter genes in chronic diseases. Mutat Res 2007;622:84–93. [PubMed: 17374385]

13. Bush AI, Pettingell WH, Multhaup G, Paradis Md, Vonsattel J-P, Gusella JF, Beyreuther K, Masters CL, Tanzi RE. Rapid induction of Alzheimer AB amyloid formation by zinc. Science 1994;265:1464–1467. [PubMed: 8073293]

14. Cherny RA, Atwood CS, Xilinas ME, Gray DN, Jones WD, McLean CA, Barnham KJ, Volitakis I, Fraser FW, Kim YS, Huang X, Goldstein LE, Moir RD, Lim JT, Beyreuther K, Zheng H, Tanzi RE, Masters C, Bush AI. Treatment with a copper-zinc chelator markedly and rapidly inhibits beta-amyloid accumulation in Alzheimer's disease transgenic mice. Neuron 2001;30:665–676. [PubMed: 11430801]

15. Taylor CG. Zinc, the pancreas, and diabetes: insights from rodent studies and future directions. Biometals 2005;18:305–312. [PubMed: 16158221]

16. Sladek R, Rocheleau G, Rung J, Dina C, Shen L, Serre D, Boutin P, Vincent D, Belisle A, Hadjadj S, Balkau B, Heude B, Charpentier G, Hudson TJ, Monpetit A, Psheszhetsky AV, Prentki M, Posner BI, Balding DJ, Meyre D, Polychronakos C, Froguel P. A genome-wide association study identifies novel risk loci for type 2 diabetes. Nature 2007;445:881–885. [PubMed: 17293876]

17. Szpunar J. Bio-inorganic speciation analysis by hyphenated techniques. Analyst 2000;125:963–988. [PubMed: 10885060]

18. Sanz-Medel A, Montes-Bayon M, Luisa Fernandez Sanchez M. Trace element speciation by ICP-MS in large biomolecules and its potential for proteomics. Anal Bioanal Chem 2003;377:236–247. [PubMed: 12904961]

19. Paunesku T, Vogt S, Maser J, Lai B, Woloschak G. X-ray fluorescence microprobe imaging in biology and medicine. J Cell Biochem 2006;99:1489–1502. [PubMed: 17006954]

20. Ralle M, Lutsenko S. Quantitative imaging of metals in tissues. Biometals 2009;22:197–205. [PubMed: 19130257]

21. Rousseau RM. Detection limit and estimate of uncertainty of analytical XRF results. Rigaku 2001;18:33–47.

22. Fahrni CJ. Biological applications of X-ray fluorescence microscopy: exploring the subcellular topography and speciation of transition metals. Curr Opin Chem Biol 2007;11:121–127. [PubMed: 17353139]

23. Jiang P, Guo Z. Fluorescent detection of zinc in biological systems: recent development on the design of chemosensors and biosensors. Coordination Chemistry Reviews 2004;248:205–229.

24. Domaille DW, Que EL, Chang CJ. Synthetic fluorescent sensors for studying the cell biology of metals. Nat Chem Biol 2008;4:168–175. [PubMed: 18277978]

25. Hirano, T.; Kikuchi, K.; Nagano, T. zinc fluorescent probes for biological applications. In: Geddes, CD.; Lakowicz, JR., editors. Reviews in Fluorescence 2004. New York: Kluwer Academic / Plenum Publishers; 2004. p. 55-73.

26. Thompson RB. Studying zinc biology with fluorescence: Ain't we got fun? Current Opinion in Chemical Biology 2005;9:526–532. [PubMed: 16129651]

27. Morelle B, Salmon JM, Vigo J, Viallet P. Measurement of intracellular magnesium concentration in 3T3 fibroblasts with the fluorescent indicator Mag-indo- 1. Analytical Biochemistry 1994;218:170–176. [PubMed: 8053551]

28. Missiaen L, Robberecht W, Van Den Bosch L, Callewaert G, Parys JB, Wuytack F, Raeymaekers L, Nilius B, Eggermont J, De Smedt H. Abnormal intracellular Ca2+ homeostasis and disease. Cell Calcium 2000;28:1–21. [PubMed: 10942700]

29. Bozym RA, Thompson RB, Stoddard AK, Fierke CA. Measuring picomolar intracellular exchangeable zinc in PC-12 cells using a ratiometric fluorescence biosensor. ACS Chemical Biology 2006;1:103–111. [PubMed: 17163650]

30. Grynkiewicz G, Poenie M, Tsien RY. A new generation of calcium indicators with greatly improved fluorescence properties. Journal of Biological Chemistry 1985;260:3440–3450. [PubMed: 3838314]

31. Lippitsch ME, Pusterhofer J, Leiner MJP, Wolfbeis OS. Fibre-optic oxygen sensor with the fluorescence decay time as the information carrier. Analytica Chimica Acta 1988;205:1.

32. Lakowicz, JR. Principles of Fluorescence Spectroscopy. Second ed.. New York: Kluwer Academic / Plenum Publishers; 1999.

33. Dandliker WB, Kelly RJ, Dandliker J, Farquhar J, Levin J. Fluorescence polarization immunoassay. Theory and experimental method. Immunochemistry 1973;10:219–227. [PubMed: 4580370]
34. White, CE.; Argauer, RJ. Fluorescence Analysis: A Practical Approach. New York: Marcel Dekker, Inc.; 1970.
35. Fernandez-Gutierrez, A.; Munoz de la Pena, A. Determinations of inorganic substances by luminescence methods. In: Schulman, SG., editor. Molecular Luminescence Spectroscopy, Part I: Methods and Applications. Vol. vol. 77. New York: Wiley- Interscience; 1985. p. 371-546.
36. Lakowicz JR, Gryczynski I, Gryczynski Z, Dattelbaum JD. Anisotropy-based sensing with reference fluorophores. Analytical Biochemistry 1999;267:397–405. [PubMed: 10036147]
37. Frederickson CJ, Kasarskis EJ, Ringo D, Frederickson RE. A quinoline fluorescence method for visualizing and assaying histochemically reactive zinc (bouton zinc) in the brain. Journal of Neuroscience Methods 1987;20:91–103. [PubMed: 3600033]
38. Zalewski PD, Forbes IJ, Betts WH. Correlation of apoptosis with change in intracellular labile Zn(II) using Zinquin [(2-methyl-8-p-toluenesulphonamido-6-quinolyloxy)acetic acid], a new specific fluorescent probe for Zn(II). Biochemical Journal 1993;296:403–408. [PubMed: 8257431]
39. Huston ME, Haider KW, Czarnik AW. Chelation-enhanced fluorescence in 9, 10-bis(TMEDA) anthracene. Journal of the American Chemical Society 1988;110:4460–4462.
40. Burdette SC, Walkup GK, Spingler B, Tsien RY, Lippard SJ. Fluorescent sensors for Zn2+ based on a fluorescein platform: Synthesis, properties and intracellular distribution. Journal of the American Chemical Society 2001;123:7831–7841. [PubMed: 11493056]
41. Gee KR, Zhou ZL, Ton-That D, Sensi SL, Weiss JH. Measuring zinc in living cells. A new generation of sensitive and selective fluorescent probes. Cell Calcium 2002;31:245–251. [PubMed: 12098227]
42. Sensi SL, Ton-That D, Sullivan PG, Jonas EA, Gee KR, Kaczmarek LK, Weiss JH. Modulation of mitochondrial function by endogenous Zn2+ pools. Proceedings of the National Academy of Sciences 2003;100:6157–6162.
43. Henary MM, Wu Y, Fahrni CJ. Zinc(II)-selective ratiometric fluorescent sensors based on inhibition of excited state intramolecular proton transfer. Chemistry in Europe Journal 2004;10:3015–3025.
44. Aoki S, Kagata D, Shiro M, Takeda K, Kimura E. Metal chelation-controlled twisted intramolecular charge transfer and its application to fluorescent sensing of metal ions and anions. Journal of the American Chemical Society 2004;126:13377–13390. [PubMed: 15479094]
45. Godwin HA, Berg JM. A fluorescent zinc probe based on metal induced peptide folding. Journal of the American Chemical Society 1996;118:6514–6515.
46. Walkup GK, Imperiali B. Fluorescent chemosensors for divalent zinc based on zinc finger domains. Enhanced oxidative stability, metal binding affinity, and structural and functional characterization. Journal of the American Chemical Society 1997;119:3443–3450.
47. Marvin JS, Hellinga HW. Conversion of a maltose receptor into a zinc biosensor by computational design. Proceedings of the National Academy of Sciences 2001;98:4955–4960.
48. Miyawaki A, Llopis J, Heim R, McCaffery JM, Adams JA, Ikura M, Tsien RY. Fluorescent indicators for Ca2+ based on green fluorescent proteins and calmodulin. Nature 1997;388:882–887. [PubMed: 9278050]
49. Pearce LL, Gandley RE, Han W, Wasserloos K, Stitt M, Kanai AJ, McLaughlin MK, Pitt BR, Levitan ES. Role of metallothionein in nitric oxide signaling as revealed by a green fluorescent fusion protein. Proceedings of the National Academy of Sciences 2000;97:477–482.
50. Jensen KK, Martini L, Schwartz TW. Enhanced fluorescence resonance energy transfer between spectral variants of green fluorescent protein through zinc-site engineering. Biochemistry 2001;40:938–945. [PubMed: 11170415]
51. Qiao W, Mooney M, Bird AJ, Winge DR, Eide DJ. Zinc binding to a regulatory zinc-sensing domain monitored in vivo by using FRET. Proc Natl Acad Sci U S A 2006;103:8674–8679. [PubMed: 16720702]
52. Dongen, EMWMv; Evers, TH.; Dekkers, LM.; Meijer, EW.; Klomp, LWJ.; Merkx, M. Variation of linker length in ratiometric fluorescent sensor proteins allows rational tuning of Zn(II) affinity in the picomolar to femtomolar range. Journal of the American Chemical Society 2007;129:3494–3495. [PubMed: 17335212]

53. Meldrum NU, Roughton FJ. Carbonic anhydrase. Its preparation and properties. J Physiol 1933;80:113–142. [PubMed: 16994489]
54. Stadie H, O'Brien WC. The catalysis of the hydration of carbon dioxide and the dehydration of carbonic acid by an enzyme isolated from red blood cells. The Journal of Biological Chemistry 1933;103:521–529.
55. Liljas A, Kannan KK, Bergsten PC, Waara I, Fridborg K, Strandberg B, Carlbom U, Jarup L, Lovgren S, Petef M. Crystal structure of human carbonic anhydrase C. Nat New Biol 1972;235:131–137. [PubMed: 4621826]
56. Hakansson K, Carlsson M, Svensson LA, Liljas A. Structure of native and apo carbonic anhydrase II and structure of some of its anion-ligand complexes. Journal of Molecular Biology 1992;227:1192–1204. [PubMed: 1433293]
57. Christianson DW, Fierke CA. Carbonic anhydrase - Evolution of the zinc binding site by nature and by design. Accounts of Chemical Research 1996;29:331–339.
58. McCall KA, Huang C, Fierke CA. Function and mechanism of zinc metalloenzymes. J Nutr 2000;130:1437S–1446S. [PubMed: 10801957]
59. Kimber MS, Pai EF. The active site architecture of Pisum sativum beta-carbonic anhydrase is a mirror image of that of alpha-carbonic anhydrases. EMBO Journal 2000;19:1407–1418. [PubMed: 10747009]
60. Kiefer LL, Krebs JF, Paterno SA, Fierke CA. Engineering a cysteine ligand into the zinc binding site of human carbonic anhydrase II. Biochemistry 1993;32:9896–9900. [PubMed: 8399158]
61. Ippolito JA, Baird TT Jr. McGee SA, Christianson DW, Fierke CA. Structure-assisted redesign of a protein-zinc-binding site with femtomolar affinity. Proc Natl Acad Sci U S A 1995;92:5017–5021. [PubMed: 7761440]
62. Kiefer LL, Ippolito JA, Fierke CA, Christianson DW. Redesigning the zinc binding siteof human carbonic anhydrase II: Structure of a His2Asp-Zn2+ metal coordination polyhedron. Journal of the American Chemical Society 1993;115:12581–12582.
63. Alexander RS, Kiefer LL, Fierke CA, Christianson DW. Engineering the zinc binding site of human carbonic anhydrase II: structure of the His-94-->Cys apoenzyme in a new crystalline form. Biochemistry 1993;32:1510–1518. [PubMed: 8431430]
64. Kiefer LL, Fierke CA. Functional characterization of human carbonic anhydrase II variants with altered zinc binding sites. Biochemistry 1994;33:15233–15240. [PubMed: 7803385]
65. Lesburg CA, Huang C, Christianson DW, Fierke CA. Histidine --> carboxamide ligand substitutions in the zinc binding site of carbonic anhydrase II alter metal coordination geometry but retain catalytic activity. Biochemistry 1997;36:15780–15791. [PubMed: 9398308]
66. McCall KA, Fierke CA. Probing determinants of the metal ion selectivity in carbonic anhydrase using mutagenesis. Biochemistry 2004;43:3979–3986. [PubMed: 15049705]
67. Kiefer LL, Paterno SA, Fierke CA. Hydrogen bond network in the metal binding site of carbonic anhydrase enhances zinc affinity and catalytic efficiency. Journal of the American Chemical Society 1995;117:6831–6837.
68. Huang CC, Lesburg CA, Kiefer LL, Fierke CA, Christianson DW. Reversal of the hydrogen bond to zinc ligand histidine-119 dramatically diminishes catalysis and enhances metal equilibration kinetics in carbonic anhydrase II. Biochemistry 1996;35:3439–3446. [PubMed: 8639494]
69. DiTusa CA, McCall KA, Christensen T, Mahapatro M, Fierke CA, Toone EJ. Thermodynamics of metal ion binding. 2. Metal ion binding by carbonic anhydrase variants. Biochemistry 2001;40:5345–5351. [PubMed: 11330997]
70. Hunt JA, Fierke CA. Selection of carbonic anhydrase variants displayed on phage. Aromatic residues in zinc binding site enhance metal affinity and equilibration kinetics. J Biol Chem 1997;272:20364–20372. [PubMed: 9252341]
71. Hunt JA, Ahmed M, Fierke CA. Metal binding specificity in carbonic anhydrase is influenced by conserved hydrophobic core residues. Biochemistry 1999;38:9054–9062. [PubMed: 10413479]
72. Cox JD, Hunt JA, Compher KM, Fierke CA, Christianson DW. Structural influence of hydrophobic core residues on metal binding and specificity in carbonic anhydrase II. Biochemistry 2000;39:13687–13694. [PubMed: 11076507]

73. Henkens RW, Sturtevant JM. The kinetics of the binding of Zn(II) by apocarbonic anhydrase. Journal of the American Chemical Society 1968;90:2669–2676.
74. Hunt JB, Rhee MJ, Storm CB. A rapid and convenient preparation of apocarbonic anhydrase. Anal Biochem 1977;79:614–617. [PubMed: 405888]
75. Pocker Y, Fong CTO. Inactivation of bovine carbonic anhydrase by dipicolinate: Kinetic studies and mechanistic implications. Biochemistry 1983;22:813–818. [PubMed: 6838825]
76. Outten CE, O'Halloran TV. Femtomolar sensitivity of metalloregulatory proteins controlling zinc homeostasis. Science 2001;292:2488–2492. [PubMed: 11397910]
77. Nicholls DG. Mitochondria and calcium signaling. Cell Calcium 2005;38:311–317. [PubMed: 16087232]
78. Taylor JT, Zeng XB, Pottle JE, Lee K, Wang AR, Yi SG, Scruggs JAS, Sikka SS, Li M. Calcium signaling and T-type calcium channels in cancer cell cycling. World Journal of Gastroenterology 2008;14:4984–4991. [PubMed: 18763278]
79. Breuer W, Epsztejn S, Cabantchik ZI. Iron acquired from transferrin by K562 cells is delivered into a cytoplasmic pool of chelatable iron(II). J Biol Chem 1995;270:24209–24215. [PubMed: 7592626]
80. Kress GJ, Dineley KE, Reynolds IJ. The relationship between intracellular free iron and cell injury in cultured neurons astrocytes, and oligodendrocytes. J Neurosci 2002;22:5848–5855. [PubMed: 12122047]
81. Petrat F, Rauen U, de Groot H. Determination of the chelatable iron pool of isolated rat hepatocytes by digital fluorescence microscopy using the fluorescent probe, phen green SK. Hepatology 1999;29:1171–1179. [PubMed: 10094962]
82. Woodmansee AN, Imlay JA. Quantitation of intracellular free iron by electron paramagnetic resonance spectroscopy. Methods Enzymol 2002;349:3–9. [PubMed: 11912920]
83. Rae TD, Schmidt PJ, Pufahl RA, Culotta VC, O'Halloran TV. Undetectable intracellular free copper: the requirement of a copper chaperone for superoxide dismutase. Science 1999;284:805–808. [PubMed: 10221913]
84. Lindskog S, Nyman PO. Metal-Binding Properties of Human Erythrocyte Carbonic Anhydrases. Biochim Biophys Acta 1964;85:462–474. [PubMed: 14194861]
85. McCall KA, Fierke CA. Colorimetric and fluorimetric assays to quantitate micromolar concentrations of transition metals. Anal Biochem 2000;284:307–315. [PubMed: 10964414]
86. Finney LA, O'Halloran TV. Transition metal speciation in the cell: insights from the chemistry of metal ion receptors. Science 2003;300:931–936. [PubMed: 12738850]
87. Hakansson K, Wehnert A, Liljas A. X-ray analysis of metal-substituted human carbonic anhydrase II derivatives. Acta Crystallogr D Biol Crystallogr 1994;50:93–100. [PubMed: 15299481]
88. DiTusa CA, Christensen T, McCall KA, Fierke CA, Toone EJ. Thermodynamics of metal ion binding. 1. Metal ion binding by wild-type carbonic anhydrase. Biochemistry 2001;40:5338–5344. [PubMed: 11330996]
89. Hunt JA, Fierke CA. Selection of carbonic anhydrase variants displayed on phage: aromatic residues in zinc binding site enhance metal affinity and equilibration kinetics. Journal of Biological Chemistry 1997;272:20364–20372. [PubMed: 9252341]
90. Maren TH. Use of inhibitors in physiological studies of carbonic anhydrase. American Journal of Physiology 1977;232:F291–F297. [PubMed: 403777]
91. Nair SK, Krebs JF, Christianson DW, Fierke CA. Structural basis of inhibitor affinity to variants of human carbonic anhydrase II. Biochemistry 1995;34:3981–3989. [PubMed: 7696263]
92. Chen RF, Kernohan JC. Combination of bovine carbonic anhydrase with a fluorescent sulfonamide. J Biol Chem 1967;242:5813–5823. [PubMed: 4990698]
93. Thompson RB, Jones ER. Enzyme-based fiber optic zinc biosensor. Analytical Chemistry 1993;65:730–734.
94. Thompson RB, Whetsell WO Jr. Maliwal BP, Fierke CA, Frederickson CJ. Fluorescence microscopy of stimulated Zn(II) release from organotypic cultures of mammalian hippocampus using a carbonic anhydrase-based biosensor system. J Neurosci Methods 2000;96:35–45. [PubMed: 10704669]

95. Thompson RB, Maliwal BP, Fierke CA. Selectivity and sensitivity of fluorescence lifetime-based metal ion biosensing using a carbonic anhydrase transducer. Anal Biochem 1999;267:185–195. [PubMed: 9918670]

96. Thompson, RB.; Maliwal, BP.; Feliccia, V.; Fierke, CA. High sensitivity determination of Zn(II) and Cu(II) in vitro by fluorescence polarization. In: Cohn, GE., editor. Systems and Technologies for Clinical Diagnostics and Drug Discovery. Vol. vol. 3259. San Jose, CA: SPIE; 1998. p. 40-47.

97. Thompson RB, Patchan MW. Lifetime-based fluorescence energy transfer biosensing of zinc. Anal Biochem 1995;227:123–128. [PubMed: 7668370]

98. Frederickson CJ, Giblin LJ 3rd, Balaji RV, Masalha R, Frederickson CJ, Zeng Y, Lopez EV, Koh JY, Chorin U, Besser L, Hershfinkel M, Li Y, Thompson RB, Krezel A. Synaptic release of zinc from brain slices: factors governing release, imaging, and accurate calculation of concentration. J Neurosci Methods 2006;154:19–29. [PubMed: 16460810]

99. Forster T. Intermolecular energy migration and fluorescence (Ger.). Annalen der Physik 1948;2:55–75.

100. Thompson RB, Cramer ML, Bozym R. Excitation ratiometric fluorescent biosensor for zinc ion at picomolar levels. J Biomed Opt 2002;7:555–560. [PubMed: 12421121]

101. Wadia JS, Dowdy SF. Transmembrane delivery of protein and peptide drugs by TAT-mediated transduction in the treatment of cancer. Adv Drug Deliv Rev 2005;57:579–596. [PubMed: 15722165]

102. Kiefer LL, Paterno SA, Fierke CA. Second shell hydrogen bonds to histidine ligands enhance zinc affinity and catalytic efficiency. Journal of the American Chemical Society 1995;117:6831–6837.

103. Frederickson CJ, Koh J-Y, Bush AI. The neurobiology of zinc in health and disease. Nature Reviews Neuroscience 2005;6:449–462.

104. Li Y, Hough CJ, Suh SW, Sarvey JM, Frederickson CJ. Rapid translocation of Zn(2+) from presynaptic terminals into postsynaptic hippocampal neurons after physiological stimulation. J Neurophysiol 2001;86:2597–2604. [PubMed: 11698545]

105. Fierke CA, Thompson RB. Fluorescence-based biosensing of zinc using carbonic anhydrase. Biometals 2001;14:205–222. [PubMed: 11831457]

106. Palm C, Netzereab S, Hallbrink M. Quantitatively determined uptake of cell-penetrating peptides in non-mammalian cells with an evaluation of degradation and antimicrobial effects. Peptides 2006;27:1710–1716. [PubMed: 16500001]

107. Dittmer PJ, Miranda JG, Gorski JA, Palmer AE. Genetically encoded sensors to elucidate spatial distribution of cellular zinc. J Biol Chem 2009;284:16289–16297. [PubMed: 19363034]

108. Vinkenborg JL, Nicolson TJ, Bellomo EA, Koay MS, Rutter GA, Merkx M. Genetically encoded FRET sensors to monitor intracellular Zn(2+) homeostasis. Nat Methods. 2009

109. Shaner NC, Patterson GH, Davidson MW. Advances in fluorescent protein technology. J Cell Sci 2007;120:4247–4260. [PubMed: 18057027]

110. Bevis BJ, Glick BS. Rapidly maturing variants of the Discosoma red fluorescent protein (DsRed). Nat Biotechnol 2002;20:83–87. [PubMed: 11753367]

111. Merzlyak EM, Goedhart J, Shcherbo D, Bulina ME, Shcheglov AS, Fradkov AF, Gaintzeva A, Lukyanov KA, Lukyanov S, Gadella TW, Chudakov DM. Bright monomeric red fluorescent protein with an extended fluorescence lifetime. Nat Methods 2007;4:555–557. [PubMed: 17572680]

112. Shaner NC, Campbell RE, Steinbach PA, Giepmans BN, Palmer AE, Tsien RY. Improved monomeric red, orange and yellow fluorescent proteins derived from Discosoma sp. red fluorescent protein. Nat Biotechnol 2004;22:1567–1572. [PubMed: 15558047]

113. Thompson RB, Maliwal BP, Feliccia VL, Fierke CA, McCall K. Determination of picomolar concentrations of metal ions using fluorescence anisotropy: biosensing with a "reagentless" enzyme transducer. Anal Chem 1998;70:4717–4723. [PubMed: 9844569]

114. Thompson RB, Maliwal BP, Zeng HH. Zinc biosensing with multiphoton excitation using carbonic anhydrase and improved fluorophores. J Biomed Opt 2000;5:17–22. [PubMed: 10938761]

115. Elbaum D, Nair SK, Patchan MW, Thompson RB, Christianson DW. Structure-based design of a sulfonamide probe for fluorescence anisotropy detection of zinc with a carbonic anhydrase-based biosensor. Journal of the American Chemical Society 1996;118:8381–8387.

116. Bozym R, Hurst TK, Westerberg N, Stoddard A, Fierke CA, Frederickson CJ, Thompson RB. Determination of Zinc Using Carbonic Anhydrase-Based Fluorescence Biosensors. Fluorescence Spectroscopy 2008;450:287–309.

117. Stumm, W.; Morgan, JJ. Third ed.. New York: Wiley-Interscience; 1996. Aquatic Chemistry: Chemical Equilibria and Rates in Natural Waters.

118. Brand LE, Sunda WG. Reduction of marine phytoplankton reproduction rates by copper and cadmium. Journal of Experimental Marine Biological Ecology 1986;96:225–250.

119. Martin M, Osborn KE, Billig P, Glickstein N. Toxicities of ten metals to Crassostrea gigas and Mytilus edulis embryos and Cancer magister larvae. Marine Pollution Bulletin 1981;12:305–308.

120. Moffett JW, Brand LE, Croot PL, Barbeau KA. Cu speciation and cyanobacterial distribution in harbors subject to anthropogenic Cu inputs. Limnology and Oceanography 1997;42:789–799.

121. Thompson, RB.; Zeng, HH.; Fierke, CA.; Fones, G.; Moffett, J. Real-time in situ determination of free Cu(II) at picomolar levels in sea water using a fluorescence lifetime-based fiber optic biosensor. In: Cohn, GE., editor. Clinical Diagnostic Systems: Technologies and Instrumentation. Vol. vol. 4625. San Jose, CA: Society of Photooptical Instrumentation Engineers; 2002. p. 137-143.

122. Thompson RB, Ge ZF, Patchan M, Huang CC, Fierke CA. Fiber optic biosensor for Co(II) and Cu (II) based on fluorescence energy transfer with an enzyme transducer. Biosensors & Bioelectronics 1996;11:557–564.

123. Thompson, RB.; Ge, Z.; Patchan, MW.; Fierke, CA. Energy transfer-based fiber optic metal ion biosensor. In: Lakowicz, JR., editor. SPIE Conference on Advances in Fluorescence Sensing Technology II. Vol. vol. 2388. San Jose, CA: SPIE; 1995. p. 138-147.

124. van den Berg C. Determining the copper complexing capacity and conditional stability constants of complexes of copper (II) with natural organic ligands in seawater by cathodic stripping voltammetry of copper-catechol complex ions. Marine Chemistry 1984;15:1–18.

125. Belli SL, Zirino A. Behavior and calibration of the copper(II) ion-selective electrode in high chloride media and marine waters. Analytical Chemistry 1993;65:2583–2589.

126. Bruland KW, Rue EL, Donat JR, Skrabal SA, Moffat JW. Intercomparison of voltammetric techniques to determine the chemical speciation of dissolved copper in a coastal seawater sample. Analytica Chimica Acta 1999;405:99–113.

127. Zheng Y, Cao X, Orbulescu J, Konka V, Andreopoulos FM, Pham SM, Leblanc RM. Peptidyl fluorescent chemosensors for the detection of divalent copper. Anal Chem 2003;75:1706–1712. [PubMed: 12705606]

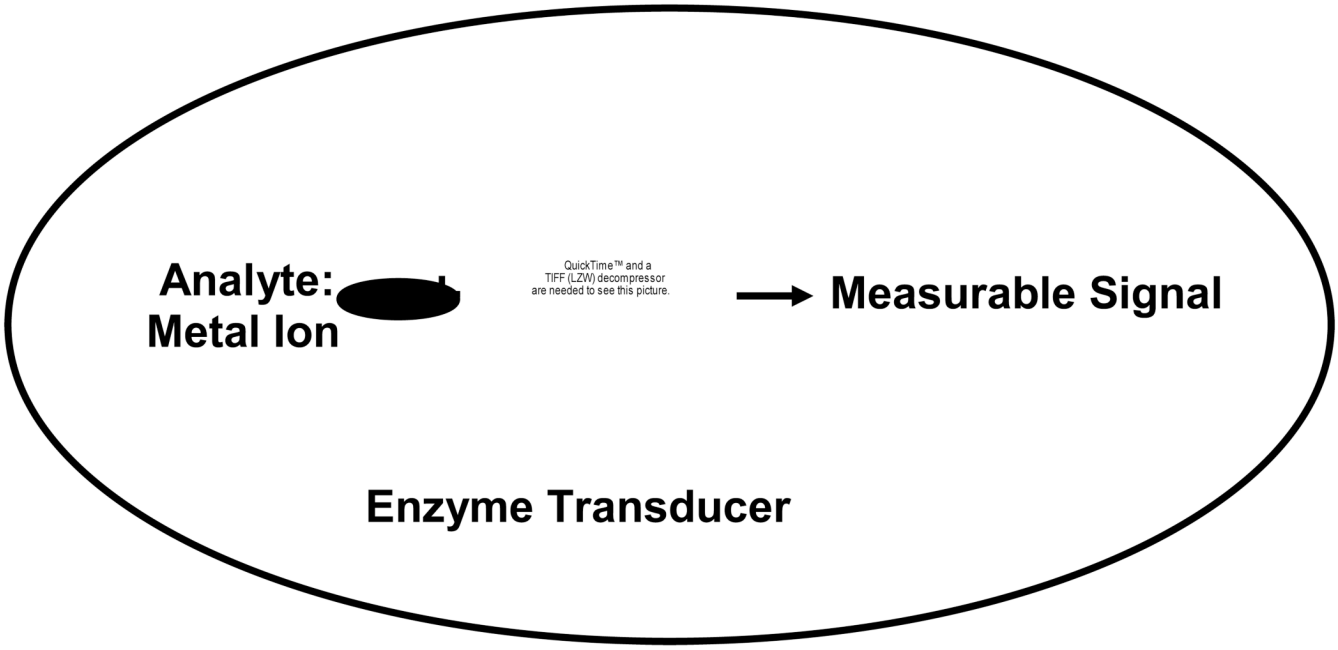

Figure 1.
Biosensor paradigm: A sensor is termed a "biosensor" if the analyte is recognized by a molecule that is biological in origin.

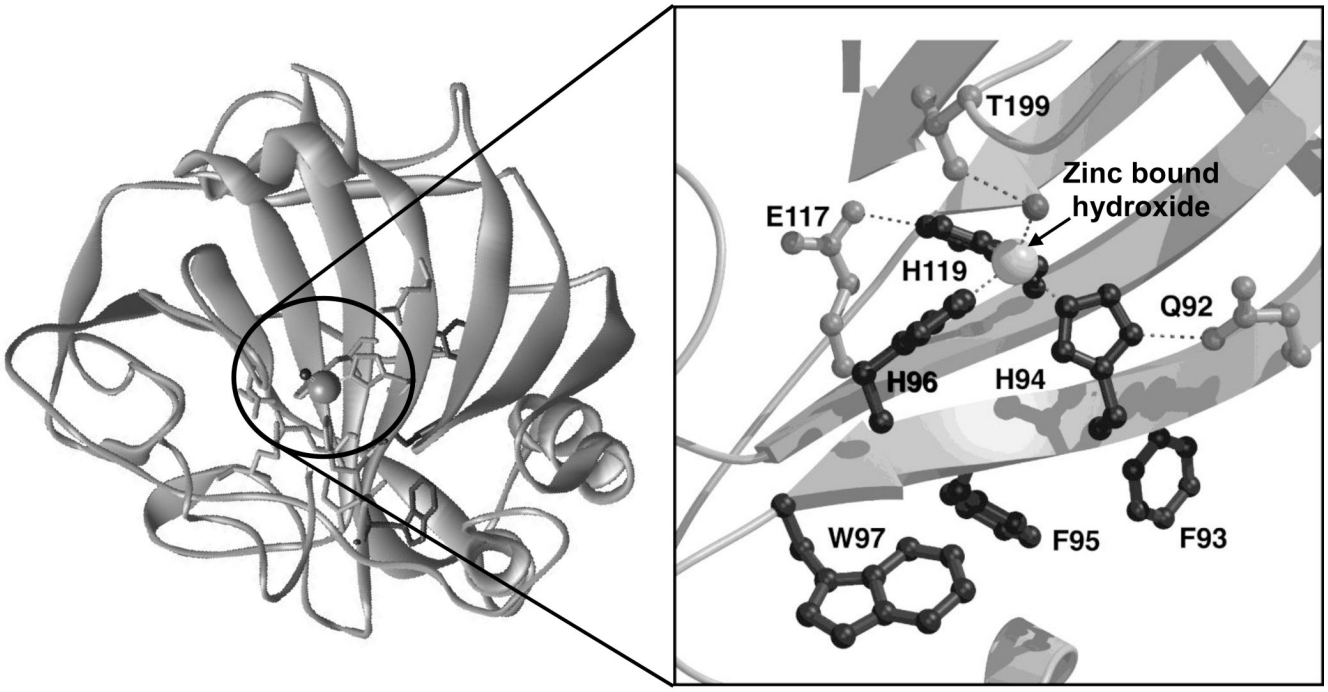

Figure 2.
Ribbon diagram of human carbonic anhydrase II: Metal binding site highlighting: the zinc ion as a sphere; the direct ligand histidines, H94, H96, H119; the second shell ligands Q92, E117, T199; and the hydrophobic residues F93, F95, W97.

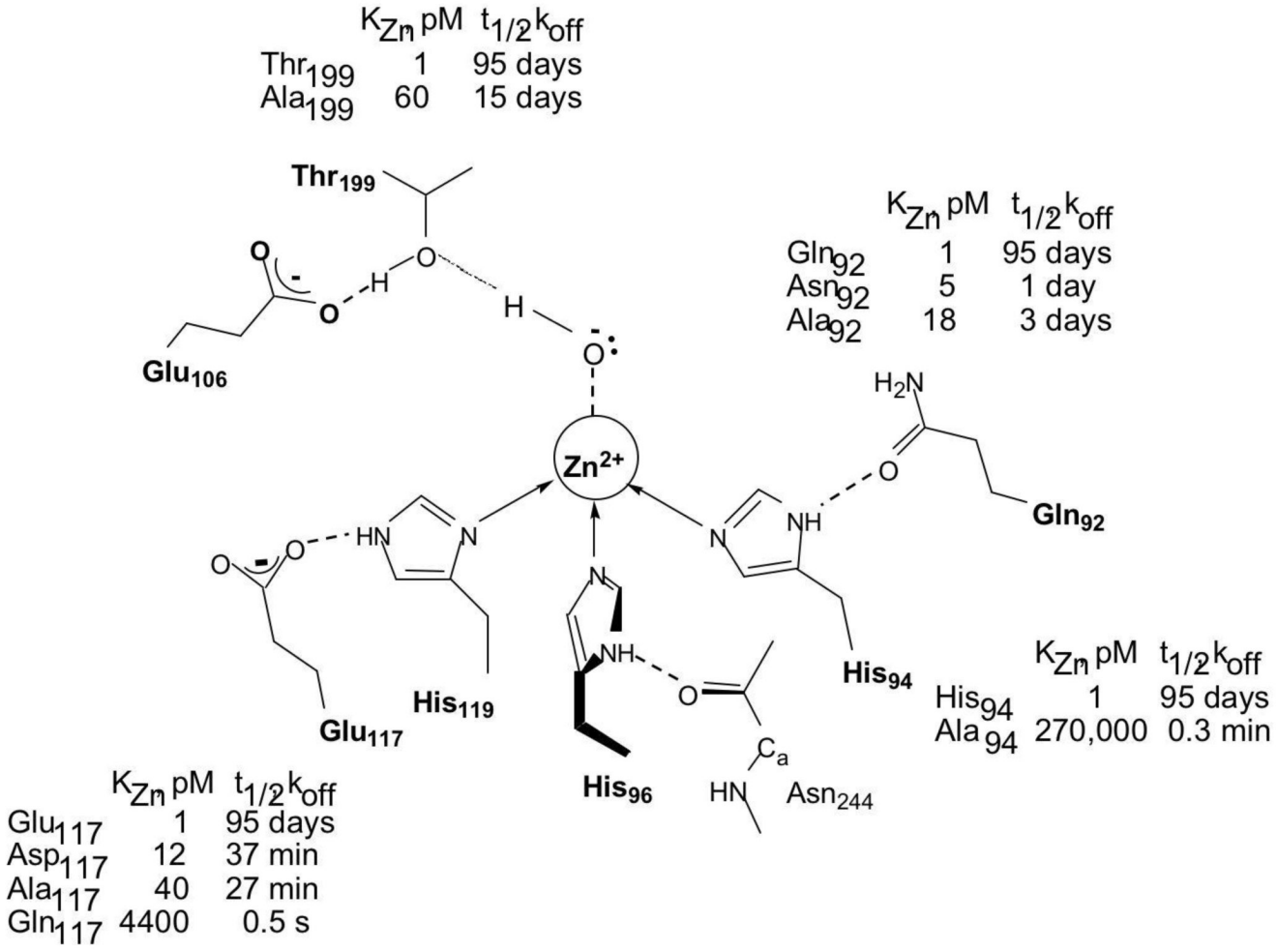

Figure 3.
Schematic diagram of the active site of WT CAII: Substitutions in both direct (H94) and indirect (E117, T199, Q92) ligands decrease the zinc affinity of CAII by 5- to 10^5 –fold, and dramatically reduce equilibration time.

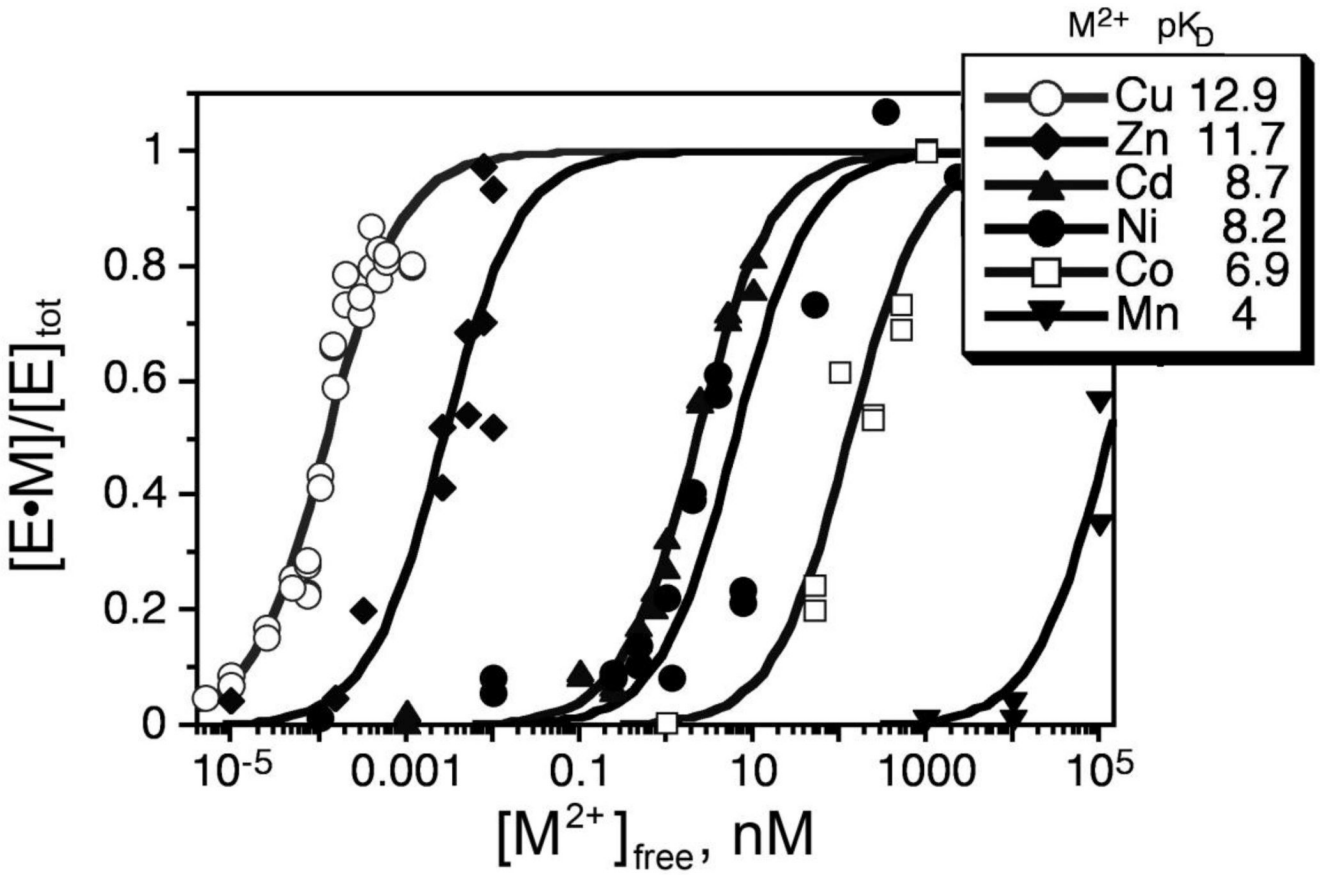

Figure 4.

Divalent metal ion affinities of WT CAII: The metal ion affinity of CAII follows the inherent metal ion-ligand affinity trend termed the Irving-William series ($Mn^{2+}<Co^{2+}<Ni^{2+}<Cu^{2+}>Zn^{2+}$).

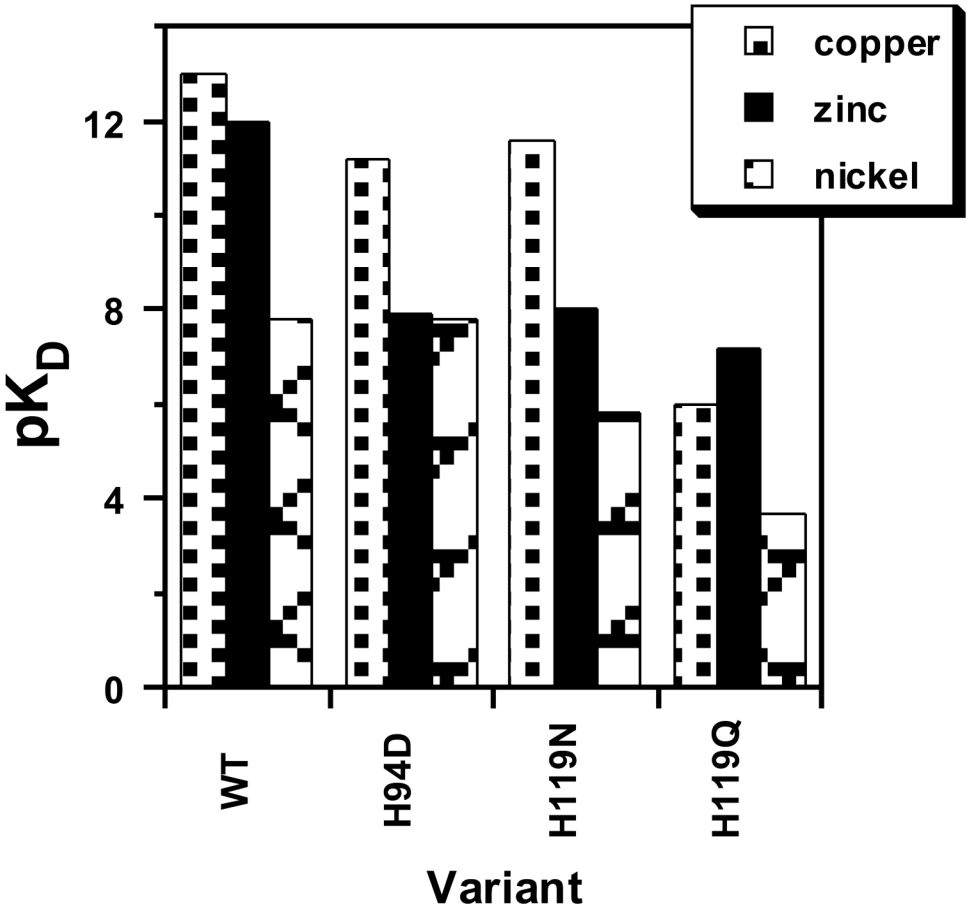

Figure 5.

Metal ion selectivity of CAII variants with mutations in the direct ligands: The affinities ($pK_D = -\log K_D$) for copper, zinc, and nickel are compared of the wild type and three variants, each with a mutation in one of the direct ligands. The Asn and Gln variants coordinate metals via an uncharged carbonyl oxygen while the Asp variant coordinates metals with a carboxylate oxygen.

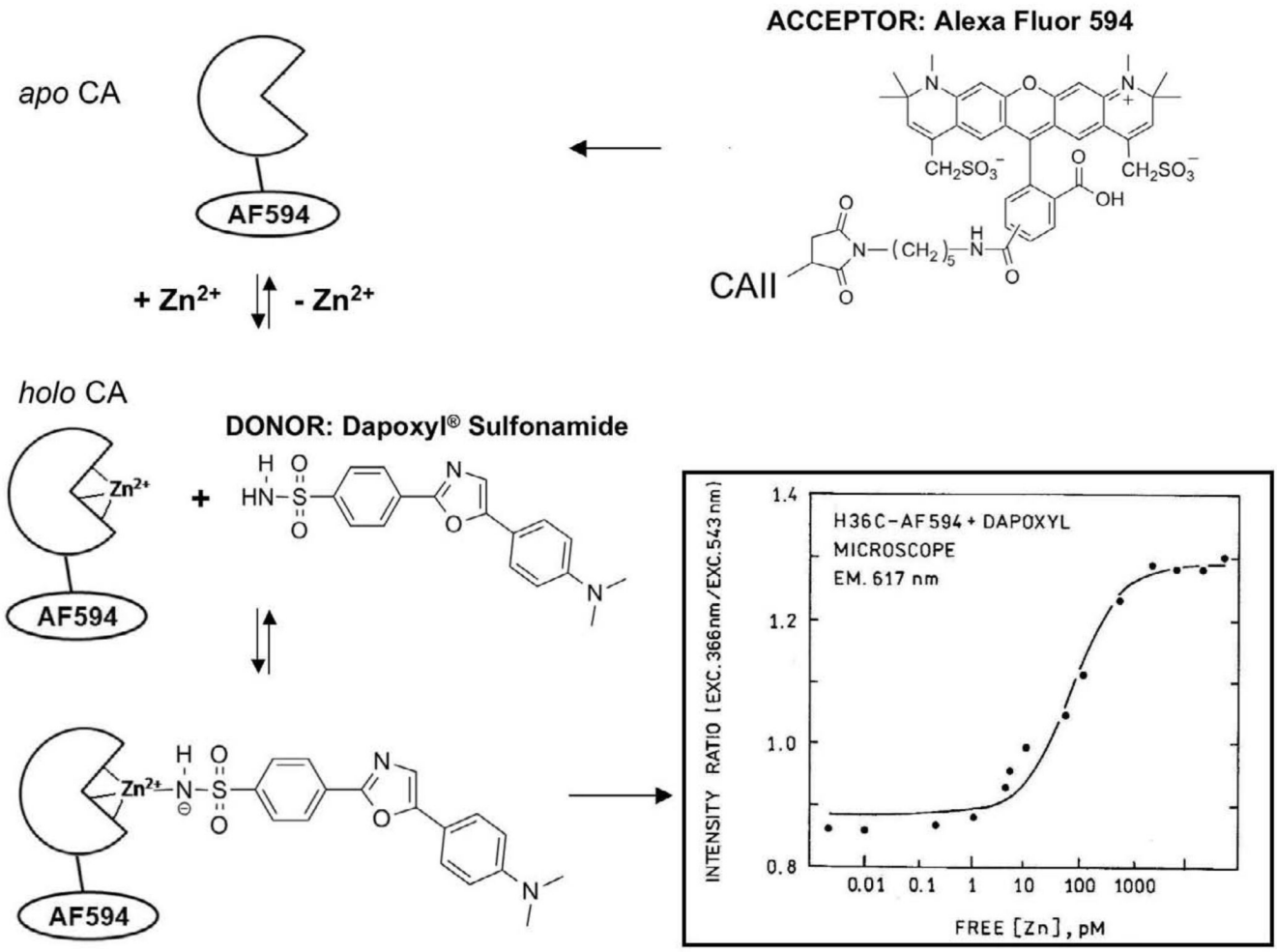

Figure 6.

FRET excitation ratiometric zinc sensing scheme: In the presence of zinc, dapoxyl sulfonamide binds to holo-CAII and transfers energy to the acceptor, AlexaFluor 594. The ratio of the acceptor fluorescence emission with excitation of the donor to that with excitation of the acceptor -is measured. The FRET intensity ratio increases with zinc concentration as the fraction of zinc-bound CAII increases, producing a binding curve with picomolar affinity (inset).

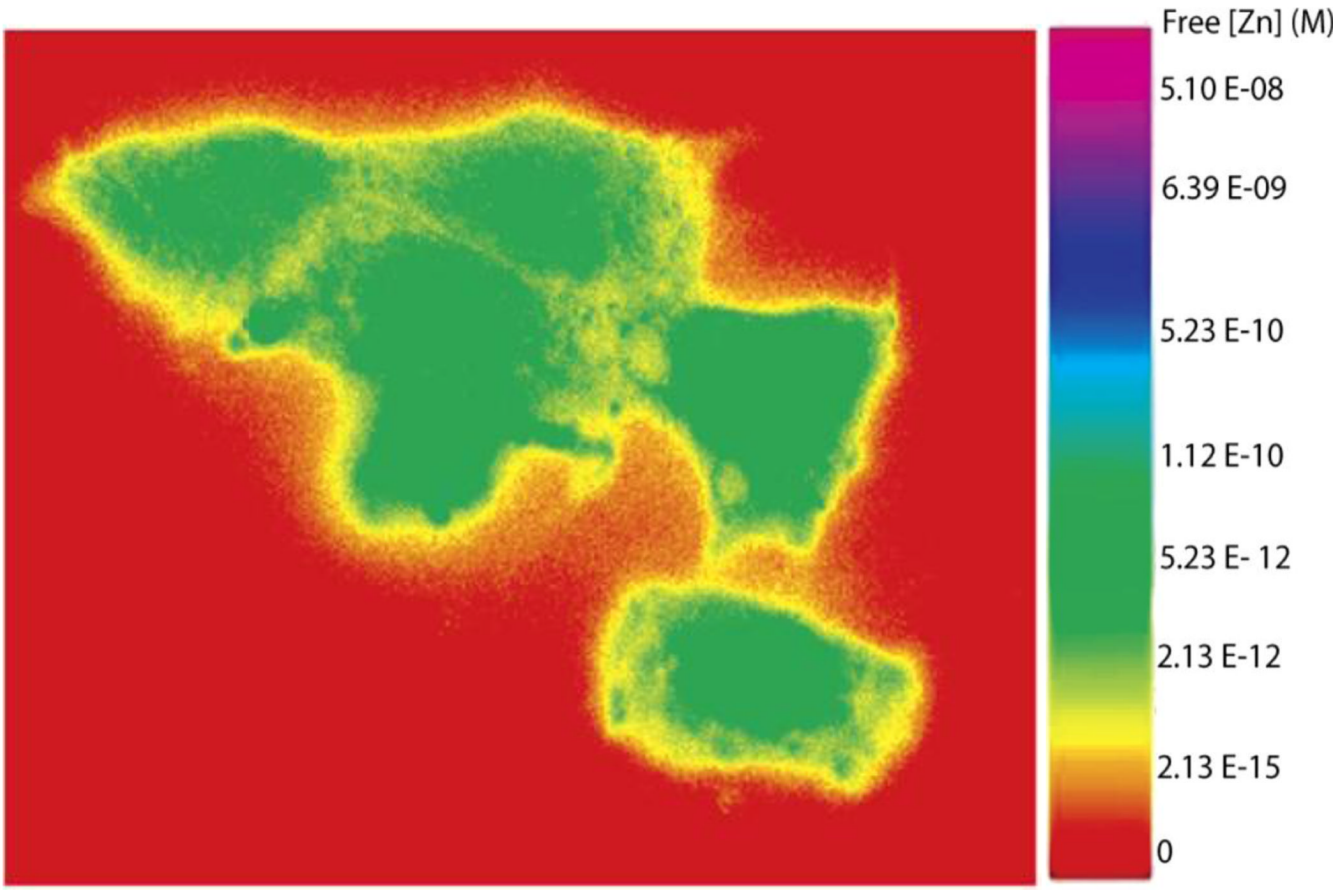

Figure 7.
False color ratio image of free zinc ion in PC-12 cells. The cells were stained with TAT-tagged H36C CAII labeled with Alexa Fluor 594 and Dapoxyl sulfonamide. The ratio image was constructed from two fluorescence micrographs taken with excitation at 380 nm, emission 617 nm; and excitation 540 nm, emission 617 nm. The calibration is measured using the same filters in the microscope with samples containing known free zinc ion concentrations maintained with NTA buffers.

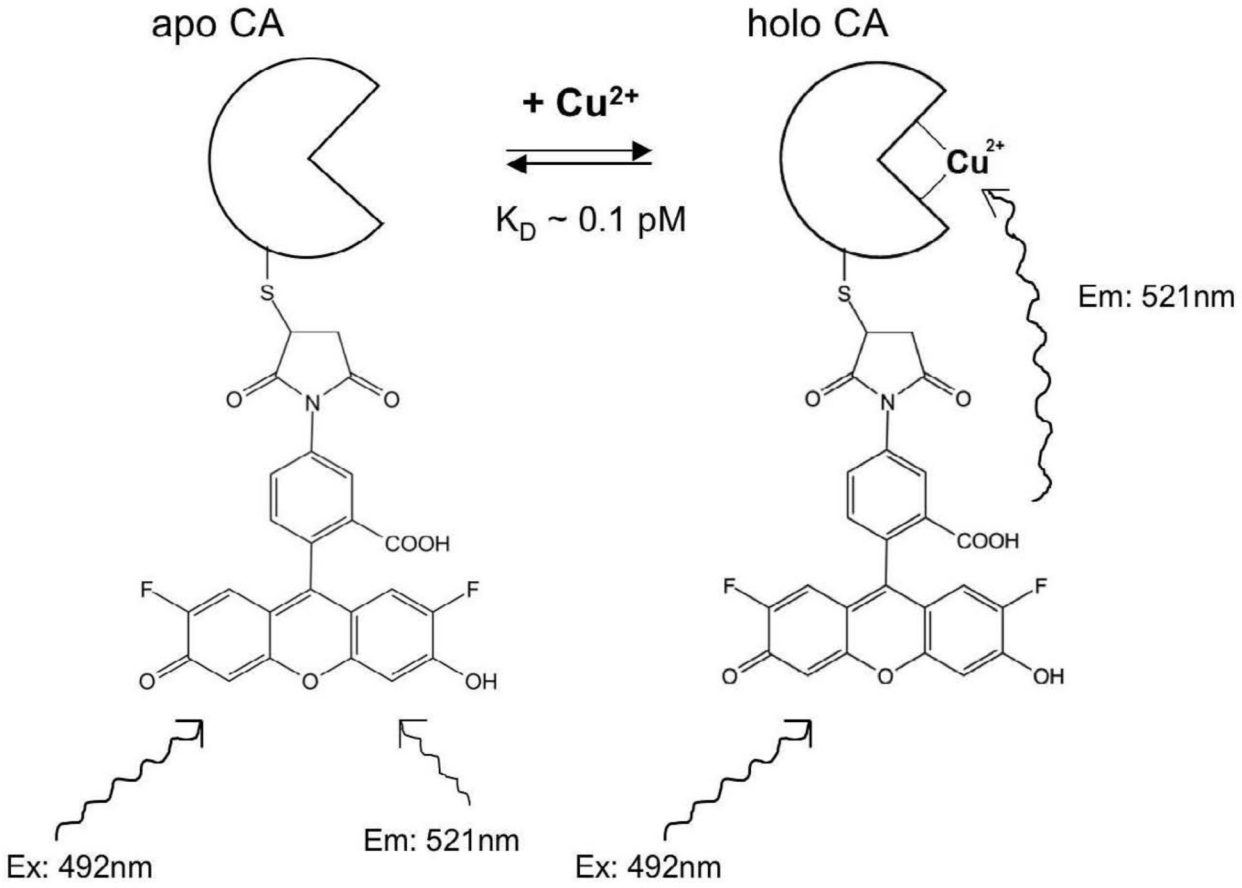

Figure 8.

Principle of CA-based fluorescence sensing of Cu^{2+}. Oregon Green maleimide is conjugated to cysteine inserted in place of a leucine (L198C) close to the active site. In the absence of Cu^{2+} (left) the Oregon Green is unquenched, but when Cu^{2+} binds in the active site the Oregon Green is partially quenched and exhibits reduced fluorescence intensity and lifetime.

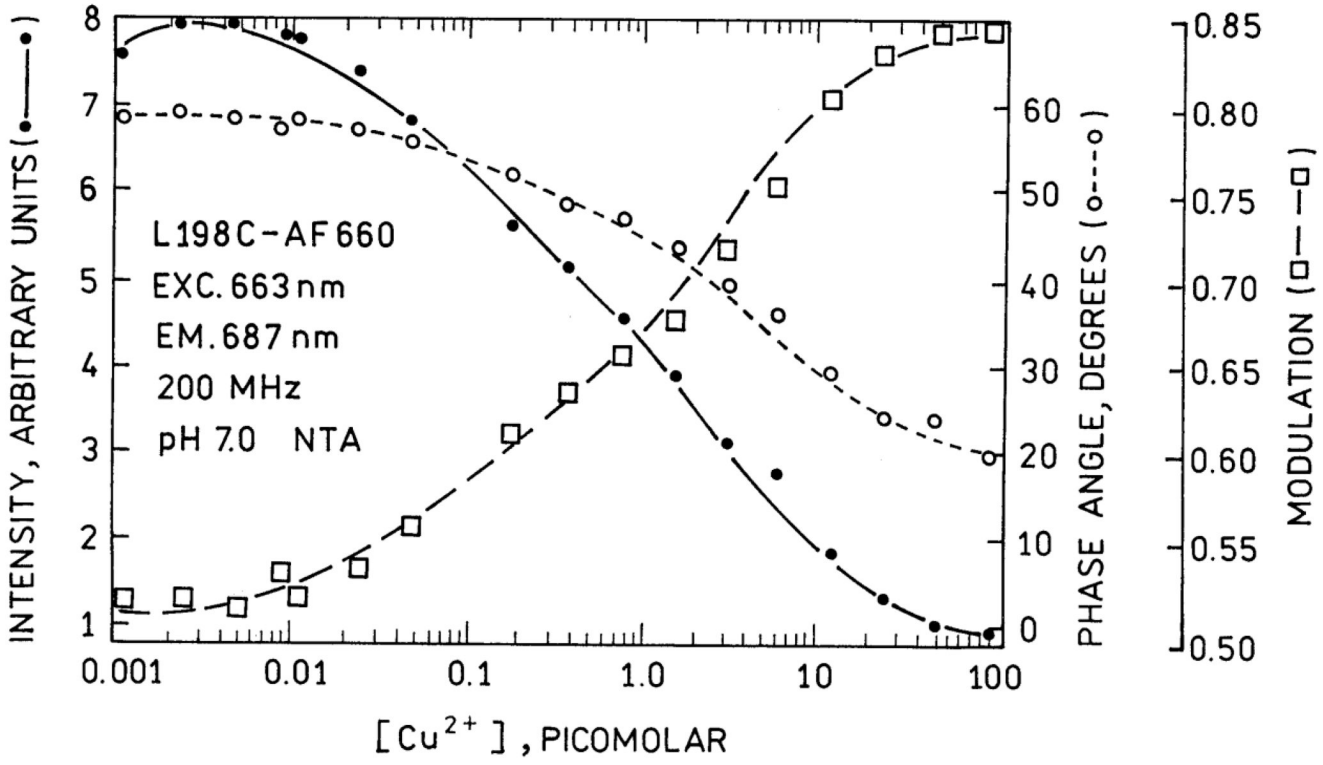

Figure 9.

Cu(II) sensor calibration. The figure depicts measured phase angles (open circles) and modulation ratios (squares) at 200 MHz (which are functions of the fluorescence lifetime) and fluorescence intensities as a function of free Cu(II) concentration in NTA buffers for L198C-apoCA II conjugated with the fluorophore Alexa Fluor 660. Reproduced with permission from Zeng, et al.

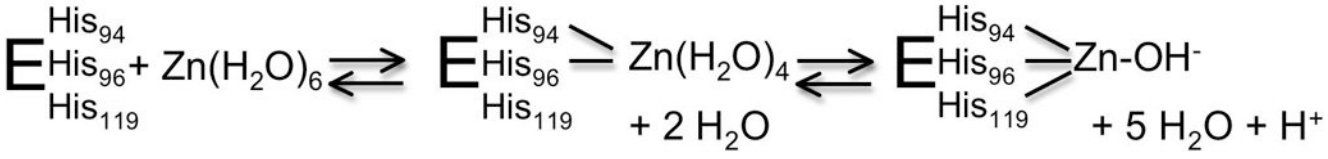

Scheme 1.
Proposed mechanism of zinc binding to CAII.

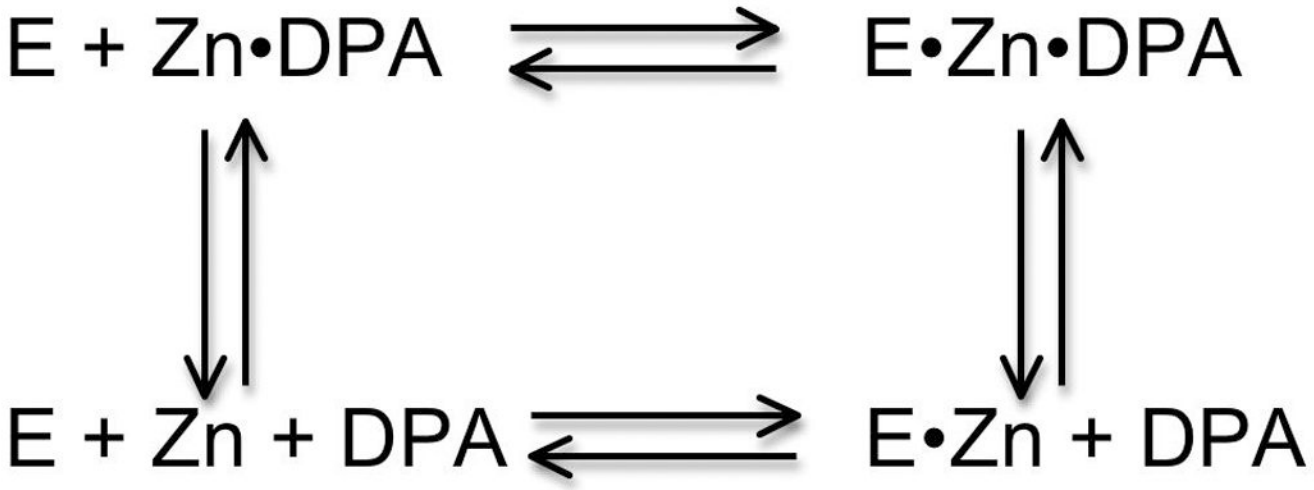

Scheme 2.
Proposed mechanism for catalysis of zinc exchange by DPA.

Table 1

Selectivity of CA: pK_D of M^{2+} of several small molecule chelators and CA.

	Mn	Co	Ni	Cu	Zn	Cd	Fe	Ca	Mg
wt CAII	<3.4	6.8	7.8	13	12	8.6*	<2	<1.3	
EDTA	14.0	16.0	18.6	18.8	16.5	16.5	14.2	10.6	8.7
EGTA	12.1	12.3	11.8	17.7	12.9	16.5	11.8	11.0	5.2
NTA	7.4	10.8	11.5	13.1	10.4	9.78	15.9	6.5	5.5
DPA	5.01	6.65	6.91	9.1	6.32	6.45	5.71	4.2	2.7
TPEN	10.3				15.6		14.6	4.4	1.7

*No affinity measurements published to date.